AIChE

A New Route for the Direct Synthesis of Al_2O_3/SiC Nanopowder Mixtures by the Carbothermal Reduction of Parent Oxides

Cavus Falamaki
Chemical Engineering Dept., Amirkabir University of Technology, Tehran, Iran; and Ceramics Dept., Materials and Energy Research Center, Tehran, Iran

Mehdi Heydarzadeh Tari and Touraj Ebadzadeh
Ceramics Dept., Materials and Energy Research Center, Tehran, Iran

DOI 10.1002/aic.11973
Published online February 1, 2010 in Wiley InterScience (www.interscience.wiley.com).

The direct synthesis of Al_2O_3/SiC nanopowders from the parent oxides Al_2O_3 and SiO_2 through mullite carbothermal reduction as intermediate phase has been investigated. The effect of the amount of excess stoichiometric carbon (active charcoal, AC) as sole carbon source on the microstructure evolution has been studied. The effect of type of carbon source (AC, graphite (G), 50 wt % AC 50 wt % G mixture, 57 wt % AC 43 wt % G mixture) on the microstructure evolution was investigated using 30 wt % excess stoichiometric carbon. The effect of reaction temperature, reaction duration, initial green compact thickness, and carbon source on the mullite conversion, morphology, and surface area of the final powders has been thoroughly investigated. The calculated activation energy is in the range of 203–230 kJ mol^{-1}, depending on the carbon source used. The synergetic effect observed for the AC/G mixtures has been accordingly explained. © 2010 American Institute of Chemical Engineers *AIChE J,* 56: 1372–1382, 2010

Keywords: carbothermal reduction, nanopowders, materials processing, microstructure mathematical modeling, green compact

Introduction

Al_2O_3/SiC composites are of high industrial interest for use in harsh applications such as high performance refractories, cutting tools, and advanced heat engines (Falamaki and Ebadzadeh, 2002). Their composites with a nanosize component do possess distinguished mechanical properties, such as high sliding wear resistance, with respect to their unreinforced counterparts (Rodriguez et al., 1999). Existing reports on the manufacture of Al_2O_3/SiC composite engineering ceramics (Na, 1999; Rodriguez et al., 1999) use nanosized Al_2O_3 and SiC powders as raw materials. The efficiency of the ''mechanical'' dispersion of the nanoparticles for the production of a homogeneous final composite is an open question when applying such mixing processes. Direct synthesis of Al_2O_3/SiC nanopowder mixtures might be a hint for obtaining a high degree of homogeneity of the components in the mixture. Although the individual synthesis of Al_2O_3 and SiC nanopowders has been the subject of intensive studies in the past, no attempt for the direct synthesis of Al_2O_3/SiC nanopowders has been reported so far. The carbothermal reduction of clay for the production of Al_2O_3 and SiC powder mixtures has been subject of few studies in the past (Bechtold and Butler, 1980; Ebadzadeh, 2002; Falamaki and Ebadzadeh, 2002). The latter works did not aim at obtaining nanopowders. This work investigates the synthesis of Al_2O_3/

Correspondence concerning this article should be addressed to C. Falamaki at c.falamaki@aut.ac.ir

Table 1. Density and Weight of a Series of Green Pellets as a Function of Thickness Using the 4/7AC-3/7G Mixture

Thickness (mm)	Weight (g)	Density (g cm^{-3})
1	0.1222	0.3892
1	0.1291	0.4111
1	0.1285	0.4092
2	0.2417	0.3849
2	0.2468	0.3930
2	0.2472	0.3936
3	0.3707	0.3935
3	0.3661	0.3886
3	0.3633	0.3857

SiC nanopowders from the parent oxides Al_2O_3 and SiO_2 through mullite carbothermal reduction as an intermediate phase. The process may be envisaged as consisting of the following two major global reactions:

$$3Al_2O_{3(solid)} + (n+2)SiO_{2(solid)} + 3nC_{(solid)} \xrightarrow{\text{heating to the reaction temperature} \geq (1400^\circ C)} Al_6Si_2O_{13(solid)} + nSiC_{(solid)} + 2nCO_{(gas)} \quad (a)$$

$$Al_6Si_2O_{13(solid)} + 6C_{(solid)} \xrightarrow{\text{reaction temperature}} 3Al_2O_{3(solid)} + 2SiC_{(solid)} + 4CO_{(gas)} \quad (b)$$

During the heating stage to the reaction temperature (reaction (a)), aluminum oxide is totally converted into mullite. As the initial green compact contains silica in excess of the stoichiometric amount for reaction (a) shown by an amount expressed in moles as n, some SiC is already present at the start of reaction (b). Actually, reaction (b) itself consists of several reactions. It is generally accepted that SiO is an intermediate gaseous species evolved throughout reaction (b) and consumed for the conversion of solid carbon into silicon carbide (Bechtold and Butler, 1980). Weimer et al. (1993) performed free energy calculations for different reaction mechanisms of the carbothermal reduction of silica in the temperature range of 1500–2500 K. According to their calculations, the most thermodynamically favorable mechanism was found as follows:

$$C_{(solid)} + SiO_{2(solid)} \rightleftarrows SiO_{(gas)} + CO_{(gas)} \quad (c)$$

$$2C_{(solid)} + SiO_{(gas)} \rightleftarrows SiC_{(solid)} + CO_{(gas)} \quad (d)$$

It is thus essential to "pelletize" to some extent the raw materials to avoid the escape of the SiO gas evolved throughout the reaction and enhance the production of a highly dispersed alumina/SiC particle system in the final product. For this means, a minimum pressure was applied just as to obtain "transportable" green compact pellets.

The key parameters for the synthesis of monophase nanopowders (like SiC) by the carbothermal reduction route are the use of fine starting materials mixed in the colloidal or molecular scale and short reaction times to inhibit crystal growth and formation of hard agglomerates (Martin et al., 1998). This article describes a new technology for obtaining a highly dispersed Al_2O_3/SiO_2 powder mixture of nanosized particles. As it will be explained in detail in what follows, a molecularly mixed powder of oxides is first prepared by a multistep procedure. The latter is heat treated at high temperatures to obtain a powder of high surface area to be used as starting material for mixing with the carbon source. An optimum reaction temperature program is then applied for the inhibition of the formation of hard agglomerates as a result of sintering phenomenon.

Experimental

Syton (X30) colloidal silica from du Pont was used as source of silica. The concentration of silica was 30 wt % with an average particle diameter of about 12 nm. Aluminum nitrate nona-hydrate (MERCK) was used as source of aluminum oxide. Deionized water was used for the preparation of the initial silica/aluminum nitrate aqueous suspension. The pH of the initial suspension was adjusted to 3 using nitric acid (65 wt %) (MERCK). Two types of carbon were used: AC (MERCK) with a specific surface area of 6.7 m^2 g^{-1} and G fine powder extra pure (MERCK) with a specific surface area of 6.11 m^2 g^{-1}.

At the very first stage, a suspension of nanosilica particles in an aqueous solution of aluminum nitrate was prepared. For this means, 51.48 g aluminum nitrate was added to 20.21 g deionized water under vigorous agitation. The pH of the solution was controlled during the dissolution process at about 3 by adding nitric acid to avoid the production of any obscurity. Afterwards, 15 g colloidal silica was added to the solution under vigorous agitation and control of pH around 3 to obtain a transparent final solution.

The obtained solution was freeze dried using liquid nitrogen at atmospheric pressure. The resulting powder was milled and calcined at 1000°C for 1 h. After cooling, the resulting powder was milled to obtain the initial nanopowder of the mixture of oxides Al_2O_3/SiO_2. According to the preparatory procedure presented, complete carbothermal reduction of the latter nanopowder should yield a composite with a weight ratio of Al_2O_3/SiC equal to 70/30. The carbon source was added to the nanopowder with the proportion of 3.51 to 10 g and the mixture was homogenized using a vibratory mixer (PE vessel with alumina balls, 15 min duration). The content of carbon in the final mixture was 30 wt % in excess of the stoichiometric amount needed for the complete reduction of oxides in the case of kinetic studies. Some experiments were performed using 5 and 50 wt % excess carbon in the case of AC. The carbon sources used were AC, G, 1/2AC-1/2G mixture (50 wt % AC, 50 wt % G), 4/7AC-3/7G mixture (57 wt % AC, 43 wt % G). The resulting mixtures were formed into disk-shaped green compacts (20 mm diameter) by uniaxial compaction (10 kN). Disks with 1, 2, and 3 mm thickness were produced by always applying the constant compaction force of 10 kN to obtain an approximately constant porosity of the green compacts independent of thickness. Table 1 shows the density of six green compacts (4/7AC-3/7G) produced with different thicknesses. It is observed that there exists no significant change in density due to increased thickness. For obtaining 1 mm thickness, about 0.12 g initial powder was needed. The green compacts were put in ceramic containers (boats) with a loosely sitting cap and the whole was put in a

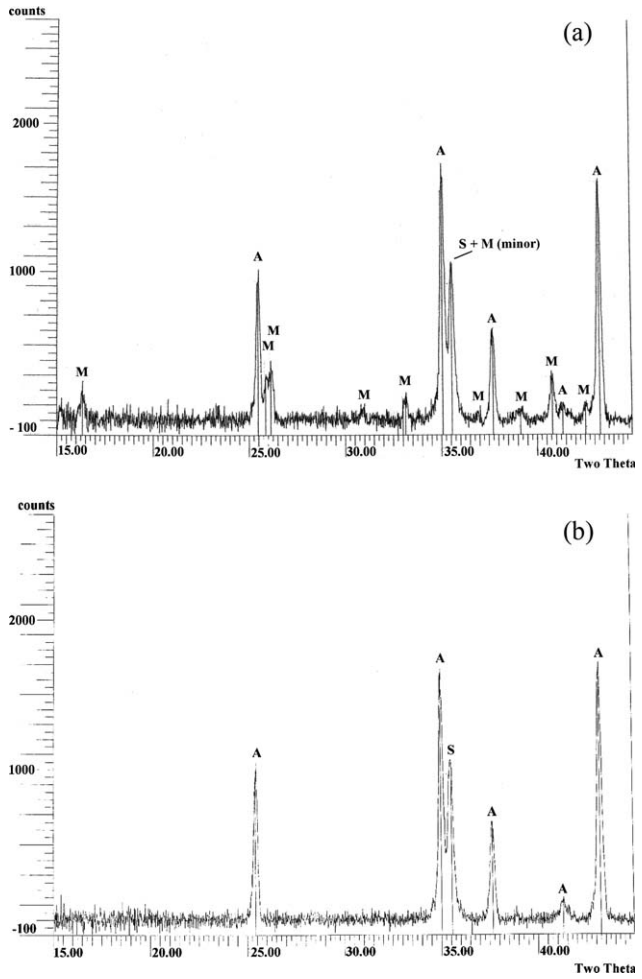

Figure 1. (a) XRD pattern of a 2-mm sample reacted at 1500°C for 60 min using 30 wt % excess AC. M, mullite; A, alpha-alumina; S, beta-SiC; (b) XRD pattern of a 1-mm sample reacted at 1500°C for 45 min using 30 wt % excess 1/2AC-1/2G. A, alpha-alumina; S, beta-SiC.

controlled atmosphere (Ar, 2 l min^{-1} flow rate) tube furnace. The samples were heated up to 1000°C with a heating rate of 10°C min^{-1} and up to the predetermined synthesis temperature (1400, 1450, and 1500°C) with a heating rate of 3°C min^{-1}. The isothermal reaction was performed applying durations of 30, 45, and 60 min. Afterwards heating was stopped and the furnace was allowed to cool down with a rate about 5°C min^{-1}. The narrow temperature range of 1400–1500°C was selected due to two reasons: (1) temperatures lower than 1400°C have a relative slow kinetics resulting in considerable amount of not-converted mullite in the final product and (2) Temperatures higher than 1500°C lead to excessive sintering, loss of surface area, and particle size increase. The Ar gas was deprived from any oxygen impurity by letting it flow through a bed of copper chips at 400°C prior entering the furnace. The resulting samples (as-synthesized samples) were then heated in a conventional electrical furnace at 800°C for 150 min for exclusion of any residual carbon (calcined samples). The weight and geometrical dimensions of the disks were measured prior and after synthesis. The amount of residual carbon was calculated in each case by measuring the weight loss during calcination.

Phase analysis of the product samples was performed using a D-500 Siemens instrument using Cu Kα radiation (wave length = 1.542 Å). The SEM analysis was done using a Stereo Scan 360-Leica (Cambridge Instruments) apparatus. The same instrument was used for X-ray microanalysis. BET surface area determination was performed using a Micromeritics Gemini 2375 (Norcross, GA) instrument using nitrogen adsorption at −195.8°C and a maximum relative pressure of nitrogen equal to 0.4.

First, the effect of amount excess stoichiometric carbon using active charcoal (AC) as sole carbon source on the microstructure evolution has been investigated. Then, the same was investigated using AC, graphite (G), AC/G mixtures at 30 wt % excess stoichiometric carbon. Based on scanning electron microscopy (SEM) and Brunauer-Emmet-Teller isotherm analysis (BET analysis), an appropriate mechanism for the microstructure evolution as a function of carbon source has been developed. The effect of reaction temperature, reaction duration, initial green compact thickness, and carbon source on the mullite conversion, morphology, and surface area of the final powders due to reactions a and b and the inherent accompanied sintering processes has been thoroughly investigated. Based on the experimental data, a mathematical model of the reaction system has been developed and discussed in detail.

It is well known that different carbon sources may substantially affect the carbothermal synthesis of carbides (Ebadzadeh, 2002). Moreover, the reason for the mullite conversion rate enhancement due to G addition to AC in the carbothermal reduction of clay to Al_2O_3/SiC powder mixtures (Ebadzadeh, 2002) is still an open question in the literature. The latter phenomenon along the effect of carbon source at constant excess stoichiometric carbon (30 wt %) on the kinetics of the reduction process has been explained. Finally, the optimum reaction conditions (temperature, duration, carbon source) for obtaining a nanopowder mixture are presented.

Results and Discussion

Generally, the reacted samples consisted of the three phases: alpha-alumina, beta-SiC, and mullite, albeit with in variable proportions. A sample XRD pattern pertaining to a 2 mm thickness sample reacted at 1500°C with a reaction time of 60 min using 30 wt. % excess AC is shown in Figure 1a. The main peaks belonging to alpha-alumina, mullite, and SiC have been indicated. Figure 1b shows the XRD pattern of a 4/7AC-3/7G sample of thickness 1 mm reacted at 1500°C for 45 min. It is observed that only peaks due to alpha-alumina and beta-SiC phases are present. It should be noted that the initial calcined powders were amorphous and did not show any distinct peak in their XRD pattern. Table 2 shows the integrated intensities (arbitrary unit) of the main peaks of mullite, α-alumina, and β-SiC in the XRD pattern of the calcined 4/7AC-3/7G samples reacted at different temperatures as a function of time of reaction and initial pellet thickness.

Table 2. Integrated Intensities (arbitrary unit) of the Main Peaks of Mullite, α-Alumina, and β-SiC in the XRD Pattern of the Calcined 4/7AC-3/7G Samples Reacted at Different Temperatures

Time (min)	Thickness (mm)	Temperature (°C)	M1*	M2†	M1 + M2	A‡	S§
60	1	1400	0.0033	0.0035	0.0068	0.0085	0.0109
45	1	1400	0.0023	0.0051	0.0074	0.0079	0.0093
30	1	1400	0.0011	0.0081	0.0092	0.0066	0.0068
60	2	1400	0.0016	0.0083	0.0099	0.0095	0.0099
45	2	1400	0.004	0.007	0.011	0.008	0.008
30	2	1400	0.0032	0.0139	0.0171	0.0068	0.0076
60	3	1400	0.0018	0.0106	0.0124	0.0079	0.0091
45	3	1400	0.0022	0.0117	0.0139	0.007	0.0077
30	3	1400	0.0038	0.0147	0.0185	0.0053	0.0068
60	1	1450	0.0003	0.0023	0.0026	0.0172	0.0215
45	1	1450	0.001	0.0029	0.0039	0.0117	0.0186
30	1	1450	0.0007	0.0059	0.0066	0.008	0.017
60	2	1450	0.0008	0.0083	0.0091	0.014	0.0212
45	2	1450	0.0019	0.0061	0.008	0.0098	0.0174
30	2	1450	0.0021	0.0068	0.0089	0.0071	0.0144
60	3	1450	0.0026	0.0087	0.0113	0.0115	0.0147
45	3	1450	0.0032	0.0075	0.0107	0.0092	0.0139
30	3	1450	0.003	0.0083	0.0113	0.0079	0.0121
60	1	1500	0	0	0	0.0165	0.0201
45	1	1500	0	0	0	0.014	0.0198
30	1	1500	0.0003	0.002	0.0023	0.0106	0.017
60	2	1500	0	0.0001	0.0001	0.0149	0.0192
45	2	1500	0.0004	0.0015	0.0019	0.0109	0.0181
30	2	1500	0.0012	0.0045	0.0057	0.0099	0.0152
60	3	1500	0.0002	0.0007	0.0009	0.0113	0.0189
45	3	1500	0.0012	0.0011	0.0023	0.01	0.0168
30	3	1500	0.0015	0.0062	0.0077	0.008	0.0145

*M1 is the integrated intensity of the single peak due to mullite in the range $2\theta = 15.5$–16.5.
†M2 is the integrated intensity of the double peaks due to mullite in the range $2\theta = 25.5$–26.5.
‡A is the integrated intensity of the single peak due to α-alumina in the range $2\theta = 25$–26.
§S is the integrated intensity of the single peak due to β-SiC in the range $2\theta = 35$–36.

The fraction of residual mullite in the product sample (f = residual mullite mass/initial mullite mass) after calcination for the removal of residual carbon may be calculated using the following relation:

$$f = 2.4921 - 9.1159\frac{m_c}{m_0} \quad (1)$$

where m_0 is the weight of the sample prior synthesis (g) and m_c is the amount of residual carbon in the synthesized product (g). Equation 1 has been derived considering the initial weight ratio of oxides Al_2O_3/SiO_2 and C/SiO_2 as 70/45 and 35/45, respectively. As mentioned in the experimental section, these ratios have been chosen as to obtain a weight ratio of Al_2O_3/SiC equal to 70/30 in case of complete carbothermal reduction of the initial sample. Generally, all the green compacts have a constant weight ratio of Al_2O_3/SiO_2 equal to 70/45 regardless of percent excess carbon used. The weight ratio of C/SiO_2 is a function of excess carbon and is 28.3/45.0, 35.1/45.0, and 40.5/45.0 for 5, 30, and 50 wt % excess carbon. Based on the initial mass ratios presented, the initial weight of mullite is $m_0 \cdot 0.6491$. The initial mass of SiC according to equation (a) due to excess silica may be calculated as $m_0 \cdot 0.0702$. The initial weight of carbon is calculated as $m_0 \cdot 0.2338$. The amount of carbon at the beginning of reaction (b) is calculated then as $m_0 \cdot 0.2338 - m_0 \cdot 0.0702 = m_0 \cdot 0.1636$. The amount of carbon reacted to convert mullite in reaction (b) may be calculated as $m_c - m_0 \cdot 0.1636$. Therefore the weight of mullite reacted through reaction (b) is calculated as $(m_c - m_0 \cdot 0.1636) \times 5.9170$. The residual mullite is then $m_0 \cdot 0.6491 - (m_c - m_0 \cdot 0.1636) \times 5.9170$ or $m_0 \cdot 1.617 - m_c \cdot 5.917$. The fraction of residual mullite is then calculated as $(m_0 \cdot 1.617 - m_c \cdot 5.917)/m_0 \cdot 0.6491 = 2.4913$–$9.1156 \cdot m_c/m_0$ (Eq. 1).

Using Eq. 1, the values of f as a function of time, reaction temperature, green compact thickness, and carbon source have been calculated and illustrated in Figures 2a–j. Based on these figures, some preliminary deductions may be summarized as follows: (a) The reaction rate of 1/2AC-1/2G mixture is significantly faster than that of AC or G samples (consider 1500°C reaction temperature) and, therefore, a "synergetic" effect is observed for AC/G mixtures; (b) increasing the thickness of the pellets reduces the reaction rate; (c) the global process is thermally activated.

Definition of nanodimension based on specific surface area

The specific surface area of a series of the calcined samples (1 mm sample thickness in all cases) is shown in Figures 3a–c. According to Figure 3a, it is observed that a linear relationship between the surface area and residual mullite fraction exists for the carbon sources 1/2AC-1/2G. This is while the surface area is rather independent of the degree of mullite conversion in the case of AC. The surface area of the initial AC and G carbon powders is smaller than 7 $m^2\ g^{-1}$ while the surface area of the 1/2AC-1/2G calcined synthesized samples is in the range of 10–36 $m^2\ g^{-1}$. The increase in the surface area, especially during the initial period of the carbothermal reaction, is due to the fine size of the initial oxides implemented. This results in fine grain

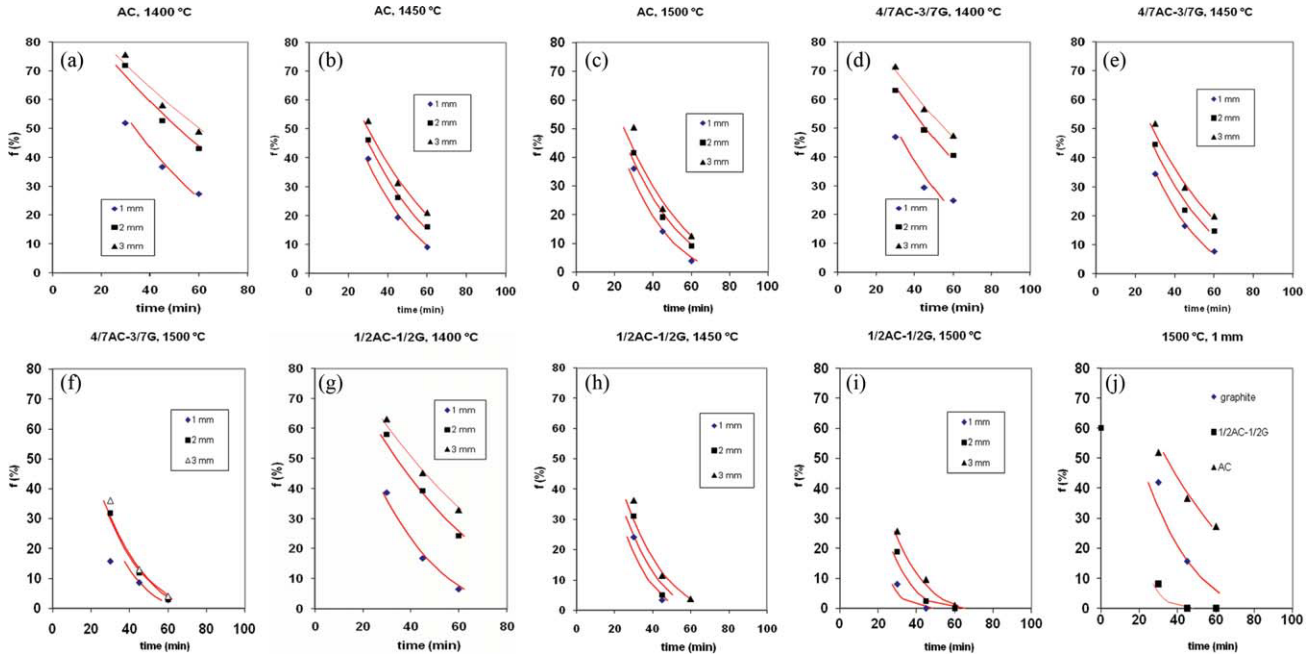

Figure 2. (a–j) *t* vs. *f* curves as a function thickness for different reaction temperatures and carbon sources (lines represent the simulated data using Eq. 4).

[Color figure can be viewed in the online issue, which is available at www.interscience.wiley.com.]

mullite particles. The surface area of the initial calcined powder of the mixed oxides has been measured to be larger than 23 $m^2\ g^{-1}$. As it will be discussed, the equivalent particle diameter of the latter is smaller than 100 nm.

Figure 3b shows the variation of surface area of the 1/2AC-1/2G samples with synthesis time for different reaction temperatures. A clear trend change is observed from 1400°C to higher temperatures. While at 1400°C the trend is quasi-linear, at higher temperatures a minimum in the curve is observed. The latter trend is shown to exist for the carbon sources G and 1/2AC-1/2G at 1500°C (Figure 3c). The surface area decreases between 30 and 45 min and increases between 45 and 60 min reaction duration. This will be discussed in the next section explaining the microstructure evolution.

The spherical equivalent diameter of the calcined synthesized powders (D_{avg}) may be calculated using the simple following relation:

$$D_{avg} = \frac{6}{\rho S_{BET}} \tag{2}$$

where ρ is the density of the powder and S_{BET} is the BET specific surface area. Powders having a spherical equivalent diameter smaller than 100 nm will be alluded to as ''nanopowders'' from now on. The results are shown in Figures 4a–c. Based on these figures and Figures 2a–j, it is observed that it is possible to produce Al_2O_3/SiC nanopowders using G and 1/2AC-1/2G carbon sources only at 1500°C and with a reaction duration of 1 h. Lower temperatures do not result in Al_2O_3/SiC nanopowders. This will be more explained in the following section covering the proposed mechanism for the microstructure evolution. For the sake of brevity, the following discussion covers only the reaction temperature of 1500°C. The mechanisms proposed are partly based on the pioneering works of Weimer et al. (1993) and Berger et al. (1999).

A complementary note should be added to clarify the definition made for the ''nanopowders.'' Referring to Figure 5, it is observed that the powder shown (50 wt % excess carbon, AC, 1500°C, 1 h) consists of agglomerates of about 0.5 μm quasi-spherical particles. Referring to the same figure, it may be observed that each of the quasi-spherical particles is made up of nanosize particles. The powder may be considered a nanopowder if the micron-size agglomerates break upon applying mechanical shear stress. For performing the BET analysis for the evaluation of the specific surface area, each powder was comminuted by grinding gently in an agata mortar to break up the ''soft'' agglomerates. The success in the breakage of the initial powder agglomerate particles into the constituent nanoblocks may be assessed by considering the absolute magnitude of the measured specific surface and also comparing it with the specific surface of the powder before grinding. Figure 5b shows an SEM picture of a fraction of an initial green compact with 30 wt % graphite as carbon source.

Microstructure evolution

AC as Sole Carbon Source (5 wt % Excess Stoichiometric Content (5ESC System), 1500°C Reaction Temperature). At this level of excess carbon, alumina and silicon carbide do exist as separate particle agglomerates. The alumina particle agglomerates consist of crystalline alpha-alumina particles embedded in an alumina amorphous matrix. Figure 6 shows the SEM picture of such agglomerates. X-ray microanalysis mode of the SEM showed that only Al is present in the latter entities. In addition, SEM and X-ray microanalysis showed

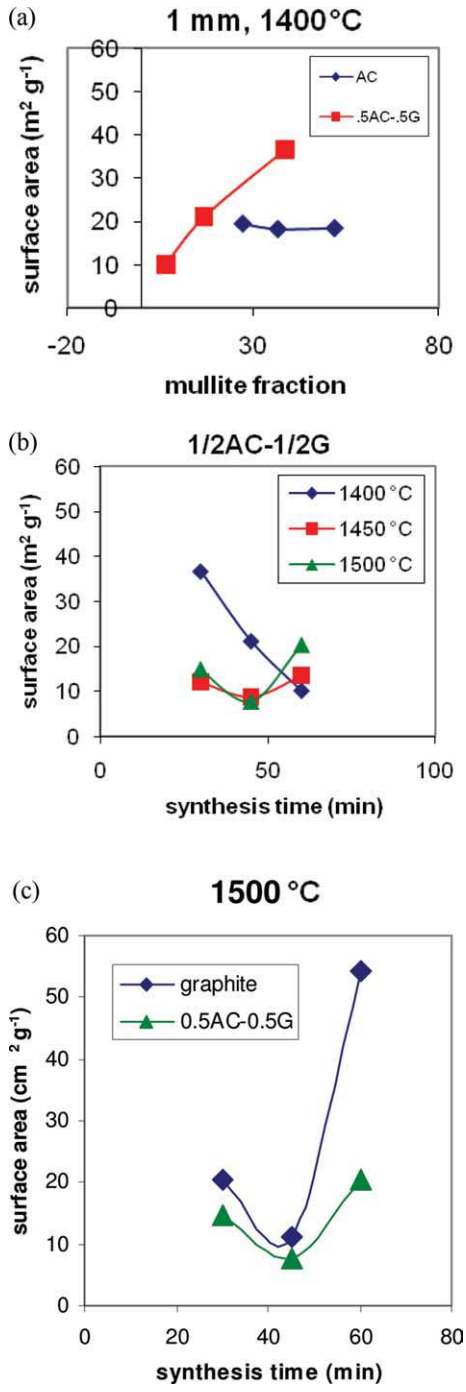

Figure 3. (a) Specific surface area of calcined final powders as a function of residual mullite fraction for AC, 1/2AC-1/2G mixture at a reaction temperature of 1400°C (1 mm thickness); (b) specific surface area of calcined final powders as a function of synthesis time for 1/2AC-1/2G mixtures at different reaction temperatures (1 mm thickness); (c) specific surface area of calcined final powders as a function of synthesis time for G, 1/2AC-1/2G mixture at a reaction temperature of 1500°C (1 mm thickness).

[Color figure can be viewed in the online issue, which is available at www.interscience.wiley.com.]

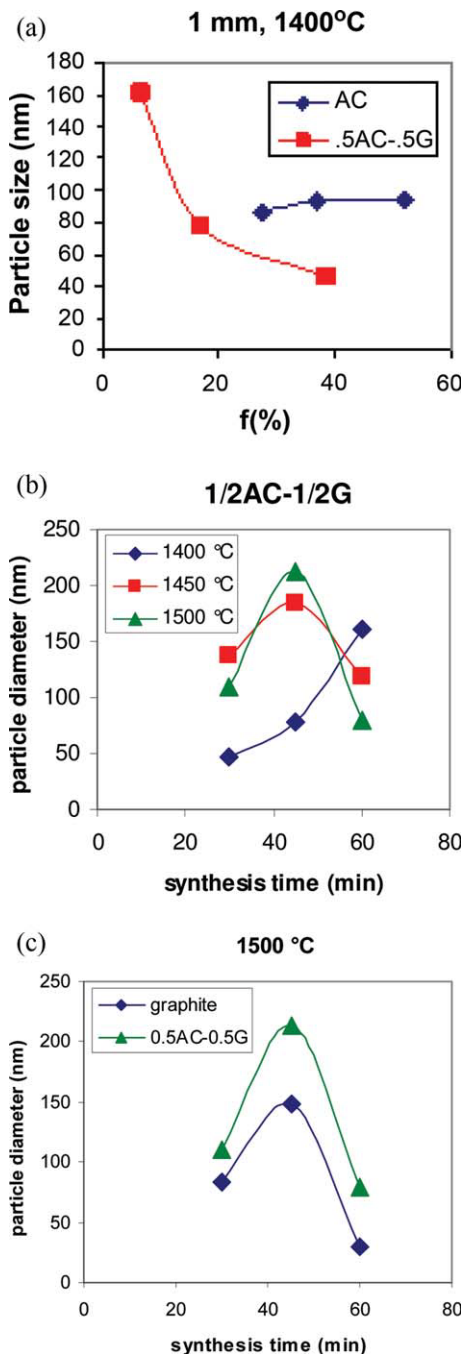

Figure 4. (a) Variation of spherical equivalent diameter as a function of residual mullite fraction for AC, 1/2AC-1/2G mixture at a reaction temperature of 1400°C (1 mm thickness); (b) variation of spherical equivalent diameter as a function of synthesis time for 1/2AC-1/2G mixtures at different reaction temperatures (1 mm thickness); (c) variation of spherical equivalent diameter as a function of synthesis time for G, 1/2AC-1/2G mixture at a reaction temperature of 1500°C (1 mm thickness).

[Color figure can be viewed in the online issue, which is available at www.interscience.wiley.com.]

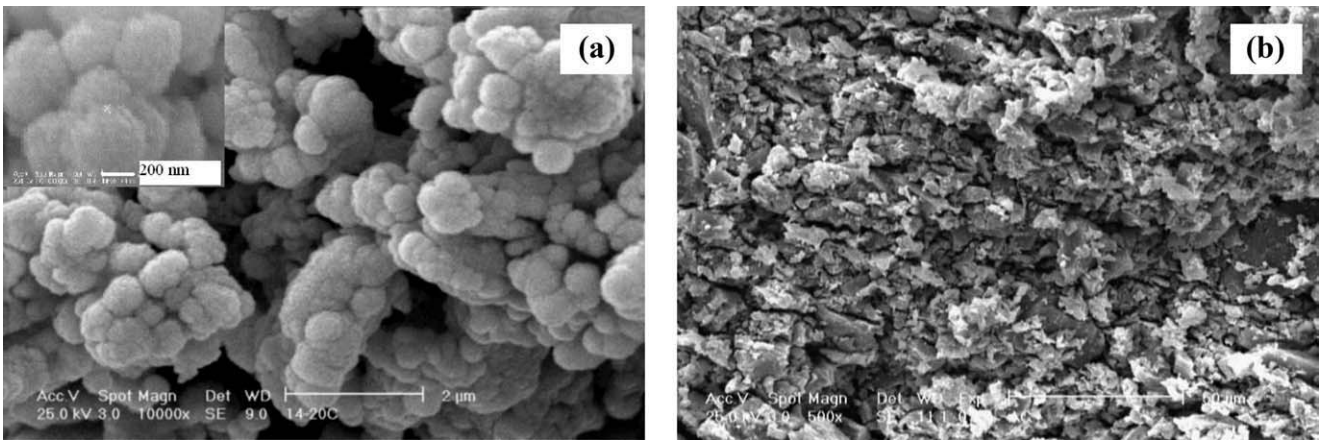

Figure 5. (a) SEM of the calcined powder synthesized at 1500°C with an inset for a higher magnifications (50 wt % excess carbon, AC, 1 h); (b) SEM of a fraction of a green compact with AC as carbon source (30 wt %).

that SiC particles form as individual particle agglomerates. The proposed mechanism for the 5ESC system is shown in Figure 7. It consists of four steps. In Step 1, aluminum and silicon oxide particles exist as nanosized particle aggregates separated from the carbon particle aggregates. This separation is merely due to the relatively low amount of excess carbon used. In Step 2, the microstructure at zero-time reaction temperature is depicted. It is observed that the initial oxides in Step 1 have been converted into separated mullite particle aggregates. The formation of some SiC particles outside the mullite aggregates has been indicated. It should be emphasized that the amount of initial SiO_2 in the green compact is more than the stoichiometric amount needed for the conversion of Al_2O_3 into mullite. The existence of "primary" SiC was confirmed by X-ray diffraction analysis. In Step 3, at the end of the reaction period, most of the mullite has been converted into alpha-alumina and SiC. SiO gas evolved during the reduction of mullite reacts outside the initial mullite particle aggregates with the carbon aggregates forming separate SiC particles. Unreacted carbon is eliminated in Step 4 upon calcination.

The alpha-alumina particle aggregates formed in Step 3 are initially porous due to the exclusion of SiO_2 in the form of SiO gas during the reduction of mullite. The high reaction temperature enhances the sintering and crystal growth of alumina. As the aggregate contains a low amount of SiC or carbon particles inside it (actually not shown), the diffusion of aluminum and oxygen atoms is not hindered and in addition to crystallization and growth, alumina particles may also form an amorphous matrix due to the abundance of alumina.

AC as Sole Carbon Source (30ESC and 50ESC Systems, 1500°C Reaction Temperature). At a 30 wt % level of excess carbon, a clear change in the morphology of particles

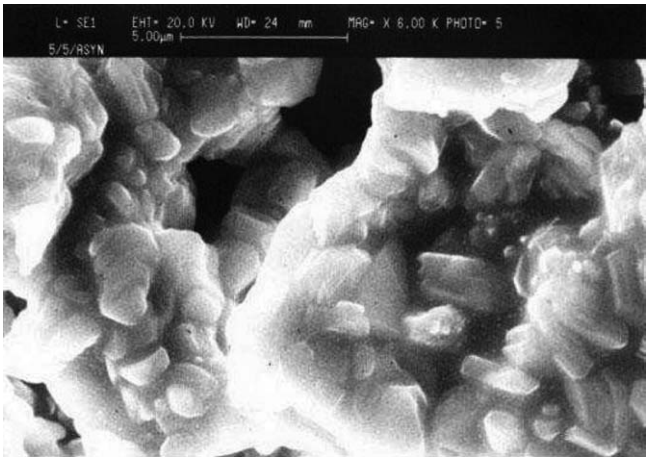

Figure 6. SEM picture of alumina particle agglomerates consisting of alpha-alumina crystals embedded in an amorphous alumina matrix (5 wt % excess AC, 1500°C, 1 h reaction time).

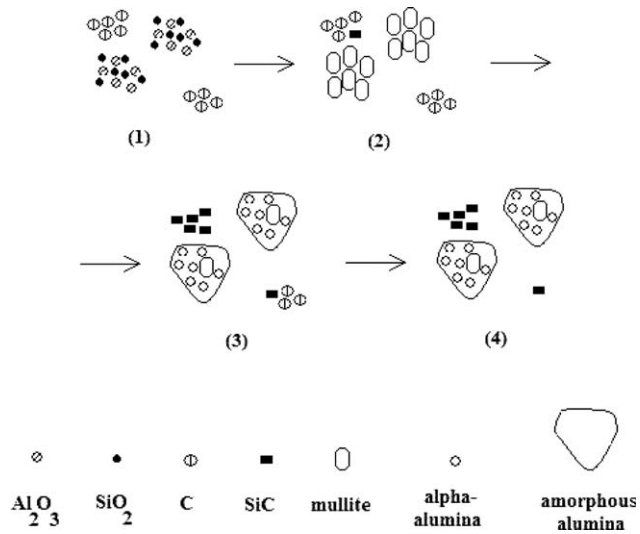

Figure 7. Proposed microstructure evolution mechanism for the case of AC as sole carbon source (5 wt % excess AC, 1500°C, 1 h reaction time).

Step 1—green compact microstructure, Step 2—at reaction temperature at zero time, Step 3—as-synthesized product at the end of the reaction time, Step 4—synthesized product after calcination. Key to the symbols is shown on the bottom.

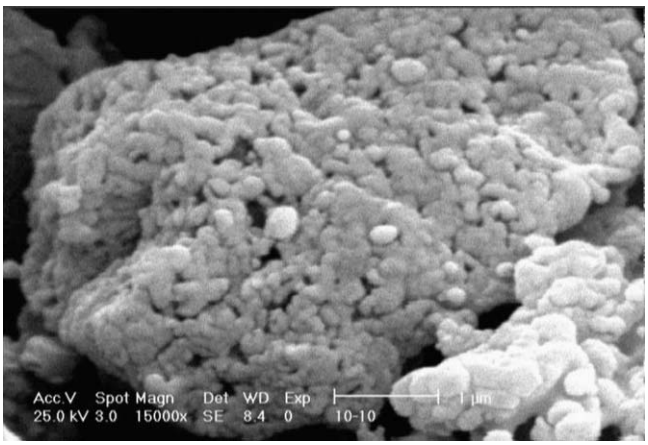

Figure 8. SEM micrograph of an alpha-alumina/SiC/mullite aggregate (30 wt % excess AC, 1500°C, 1 h reaction time).

with respect to the 5ESC system is observed. SEM and EDAX analysis showed the existence of alpha-alumina/SiC aggregates (with or without residual mullite depending on the reaction duration) and a minority of separate SiC aggregates. Figure 8 shows the micrograph of an alpha-alumina/SiC/mullite aggregate (1 h reaction time). It has internal porosity and seems to be constructed of ''glued'' very fine particles.

The proposed mechanism for the 30ESC system is shown in Figure 9. In Step 1, aluminum and silicon oxide nanoparticles coexist with carbon particles forming complex particle aggregates. The better distribution of carbon particles between the oxide particles is due to the increased carbon content. As a result, the microstructure at zero-time reaction temperature is that depicted as Step 2 in Figure 9. It is observed that the initial oxides in Step 1 have been converted into separated mullite particle aggregates. The inter-agglomerate carbon particles inhibit formation of large mullite agglomerates and induce a high surface area to it. Thus,

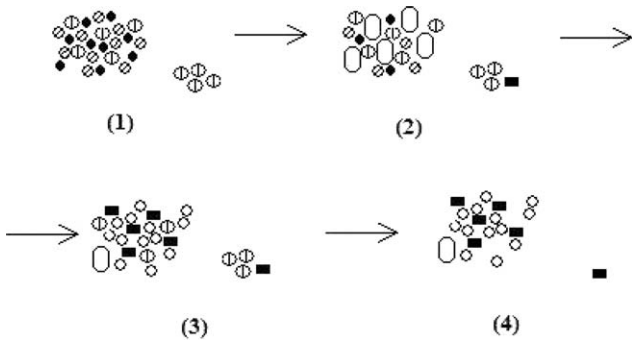

Figure 9. Proposed microstructure evolution mechanism for the case of AC as sole carbon source (30 wt % excess AC, 1500°C, 1 h reaction time).

Step 1—green compact microstructure, Step 2—at reaction temperature at zero time, Step 3—as-synthesized product at the end of the reaction time, Step 4—synthesized product after calcination. Key to the symbols is shown at the bottom of Figure 5.

at Step 2, high surface area porous aggregates consisting of mullite (mainly), carbon and some SiC particles do form. As reaction proceeds (Step 3), the latter aggregates transform into aggregates of fine alpha-alumina, SiC and unreacted carbon and mullite particles. The calcined product thus consists of two types of aggregates: alpha-alumina/SiC/(mullite, if present) and SiC. Based on SEM and EDAX analysis, increasing the excess carbon content from 30 to 50 wt %, results in a similar geometry and type of aggregates, although the aggregates are smaller in size. Figure 5 shows an SEM picture of such entities. According to the experimental data discussed earlier and the structure evolution mechanism proposed, a high degree of mixing of Al_2O_3 and SiC phases in the final product is obtained.

The trend of surface area decrease from 30 to 45 min and further increase from 45 to 60 min reaction duration at 1500°C mentioned before can be explained as follows: From 30 to 45 min, the activated sintering process decreases the surface area. From 45 to 60 min, due to the conversion of mullite, SiC particles form on the carbon particles. As explained by Berger et al. (1999), the reaction of SiO gaseous intermediate with carbon particles produces mesoporous SiC. In other words, the production of SiC at late reaction times is accompanied with an increase of total surface area which confirms the experimental results.

AC/G as Carbon Source (30ESC System, 1500°C Reaction Temperature). The microstructure evolution scheme is generally the same as that shown in Figure 9 for AC for the 30ESC system. The main difference consists in the production of a minority of SiC whiskers. This morphology has been reported by Bechtold and Butler (1980) for the carbothermal reduction of clay. They attributed the whisker morphology to the following mechanism: Existence of metal impurities like Fe, Cr, and Co in the G carbon source may induce the formation of liquid droplets of metal silicides at the mullite outer surface by the reaction of SiO gas and the metal impurity (probably in the form of oxide) on

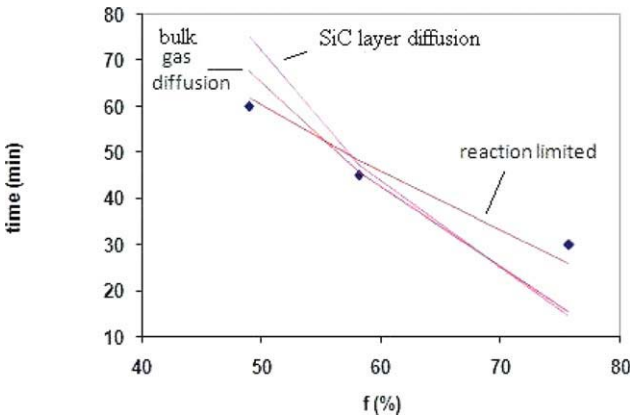

Figure 10. Different models applied to a 3 mm thickness sample reacted at 1450°C using AC as carbon source (bulk gas diffusion control: $f = 1 - \frac{1}{L}(kt)^{0.5}$, SiC layer diffusion control: $kt = 1 - 3f^{\frac{2}{3}} + 2f$, reaction control: $kt = 1 - f^{\frac{1}{3}}$).

[Color figure can be viewed in the online issue, which is available at www.interscience.wiley.com.]

Table 3. Optimum Calculated Values of k as a Function of Temperature, Pellet Thickness, and Carbon Source

Carbon Source	Temperature (°C)	Thickness (mm)	k (min^{-1})
AC	1400	1	0.0061
AC	1400	2	0.0040
AC	1400	3	0.0034
AC	1450	1	0.0091
AC	1450	2	0.0075
AC	1450	3	0.0069
AC	1500	1	0.0105
AC	1500	2	0.0091
AC	1500	3	0.0083
4/7AC-3/7G	1400	1	0.0067
4/7AC-3/7G	1400	2	0.0045
4/7AC-3/7G	1400	3	0.0037
4/7AC-3/7G	1450	1	0.0098
4/7AC-3/7G	1450	2	0.0082
4/7AC-3/7G	1450	3	0.0071
4/7AC-3/7G	1500	1	0.0123
4/7AC-3/7G	1500	2	0.0111
4/7AC-3/7G	1500	3	0.0109
1/2AC-1/2G	1400	1	0.0096
1/2AC-1/2G	1400	2	0.0061
1/2AC-1/2G	1400	3	0.0051
1/2AC-1/2G	1450	1	0.0143
1/2AC-1/2G	1450	2	0.0125
1/2AC-1/2G	1450	3	0.0111
1/2AC-1/2G	1500	1	0.02083
1/2AC-1/2G	1500	2	0.0154
1/2AC-1/2G	1500	3	0.0128

the mullite outer surface. This liquid phase further reacts with CO gas and produces columnar SiC particles. The latter carbide is attached on mullite on one end and has a liquid metal silicide droplet on the other end at the reaction temperature.

It should be stressed that the mechanisms proposed in the upper sections are mainly a theory proposed from the authors of this work that can explain all the experimental observations obtained.

Kinetic analysis

As mentioned earlier, for a constant type of carbon source, the rate of mullite conversion decreases with increasing thickness of the pellets. Such an observation induced the authors of this work to consider a priori a "diffusion controlled mechanism," along other models. Such a model has been reported previously (Falamaki and Ebadzadeh, 2002) for the carbothermal reduction of clay using disk-shaped green compacts. The model is based on the CO gas diffusion out of the pellet to be rate controlling throughout the reaction and has the simple form of:

$$f = 1 - \frac{1}{L}(kt)^{0.5} \tag{3}$$

where f is the fraction of residual mullite, L is the thickness of the disk-shaped initial sample (m), t the synthesis time (s), and k a reaction constant proportional to the gas diffusion coefficient (min^{-1}).

According to Eq. 3, the rate should decrease as the thickness is increased for a constant reaction time, in accordance with the experimental results. Based on the experimental values of f, L, and t, the unknown parameter k could be estimated to give the best fit of the data.

It was observed that Eq. 3 could reasonably predict f values for 1 mm thickness pellets (all carbon sources, all temperatures), but failed in most of the cases to predict the same for higher thicknesses with reasonable accuracy. Accordingly, the diffusion model was discarded.

Based on previous reported studies on similar processes (e.g., Weimer et al., 1993), there is great evidence that the transformation reaction of carbon to SiC by the reaction of carbon with SiO gas might be the controlling step. In this process, the size of the reacting carbon particle undergoes little change and a layer of SiC forms on the outer part of the carbon particle. The inner part of the reacting particle (core) is carbon and shrinks with time. In the absence of gas film resistance, the kinetics of such reacting particles of unchanging size may be controlled by the diffusion through the porous SiC outer layer or the chemical reaction at the surface of the unreacted core. A thorough study by the authors of this work showed that chemical reaction is the limiting step and the pertaining model could predict reasonably f as a function of time for all carbon sources, thicknesses, and reaction temperatures understudy. The model based on SiC layer diffusion control (Levenspiel, 1972) failed, especially at high thicknesses (see Figure 10).

It may be shown that for a particle of unchanging size with a shrinking inner core, the following relation between f and t holds (Levenspiel, 1972):

$$k\,t = 1 - f^{1/3} \tag{4}$$

where k is an overall rate constant and is calculated from the following equation:

$$k = \frac{k_s C_{SiO}}{\rho_c R} \tag{5}$$

where k_S is the rate constant of the assumed first-order unreacted core surface reaction, C_{SiO} is the concentration of SiO in the bulk gas phase, ρ_C is the density of the carbon particle, and R is the initial average radius of the carbon particle.

Based on the experimental values of f as a function of time, the optimum reaction constant k was determined so as to get the best fit between the experimental values of f and

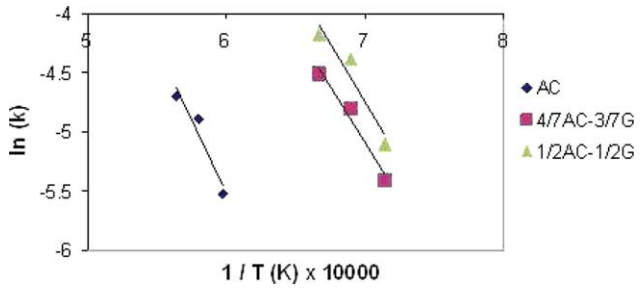

Figure 11. Arrhenius plot for 2 mm samples using different carbon sources ($k = k_0 \exp(-E/RT)$).

[Color figure can be viewed in the online issue, which is available at www.interscience.wiley.com.]

Table 4. Calculated Activation Energy as a Function of Carbon Source (2 mm thickness)

Carbon Source	Activation Energy (kJ mol^{-1})	Correlation Coefficient
AC	203	0.922
4/7AC-3/7G	223	0.970
1/2AC-1/2G	230	0.918

those predicted by Eq. 5 by minimizing the square root of the sum of the square of errors. The calculated k values are summarized in Table 3. The simulated t vs. f curves are shown in Figures 2a–j. Generally, the model predicts reasonably mullite conversion for all AC samples. The conversion of mullite for the 4/7AC-3/7G samples is also well predicted for all thicknesses up to 1450°C. At 1500°C, the behavior of the 1 mm sample is not well simulated and this is mainly attributed to experimental error in obtaining the f values. Mullite conversion is also well predicted for the 1/2AC-1/2G samples, with the exception of the 2 mm sample at 1450°C. Generally, Eq. 5 predicts reasonably mullite conversion for small and large thicknesses throughout the whole temperature range under consideration.

The Arrhenius plots based on the k values obtained for the 2 mm samples has been drawn for different carbon sources used (Figure 11) and the pertaining activation energies are listed in Table 4. The calculated activation energies are in the limited range of 203–230 kJ mol^{-1}, with an average value of 219 kJ mol^{-1}. Existing reports on the activation energy of the carbothermal reduction of silica and clay show a rather wide range of values (250–550 kJ mol^{-1}) (Weimer et al., 1993). Our result agrees to the lower level of activation energies. The relatively lower activation energy calculated in our case may be attributed to the specific type and morphology of the carbon sources used in this study.

According to Eqs. 4 and 5, the change in the value of k with increasing thickness at constant temperature and carbon source may be attributed to changes in the size of the carbon particles. As the compaction pressure applied for the forming of the initial green compacts of different thicknesses was constant (10 kN) and relatively low, it is presumed that for thicker samples, the initial carbon particles undergo less breakage upon compaction. Actually we observed that the 3 mm samples were significantly more brittle and therefore their handling was difficult. This was not the case for the 1 mm samples which showed a clear higher mechanical strength.

Actually the rheological behavior of the initial powder during the formation process (uniaxial compression) is strongly dependent on the type of carbon source used. In other words, different carbon sources result in different initial microstructures of the green compacts and different size distribution and morphology of the constituent carbon particles. The previously mentioned synergetic effect observed in the case of AC/G mixtures is attributed to the latter phenomenon. A simple possible physical explanation may be stated as follows: Graphite particles may be envisaged as lumps of two-dimensional carbon sheets. When using a mixture of G and AC as carbon sources, G sheets may slide and detach from the parent G particles due to the mechanical action of AC particles. Consequently, the average size of the carbon particles may undergo a substantial decrease, eventually resulting in a faster transformation rate. The optimum (most detached G sheets) microstructure is obtained when using a 50 wt % G and 50 wt % AC as carbon source (fastest kinetics).

Conclusions

This work discloses for the first time the direct synthesis of Al_2O_3/SiC nanopowders from the parent oxides Al_2O_3 and SiO_2 through mullite carbothermal reduction as an intermediate phase.

It has been shown that the percent excess stoichiometric amount of carbon has a major role in the microstructural evolution of the system influencing the success in obtaining nanopowders. Considering 5, 30, and 50 wt % excess carbon, the optimum amount has been determined to be 30 wt % in the case of AC as sole carbon source.

A microstructure evolution mechanism was proposed that allows the prediction of the final microstructures as a function of amount excess carbon predicting the production of high surface area powders with a high level of dispersion of the alumina and silicon carbide solid components.

It has been shown that for the direct method of synthesis of Al_2O_3/SiC nanopowder mixtures, the kinetics is reaction-limited. The activation energy of the transformation process has been calculated to be in the range of 203–230 kJ mol^{-1}. For a constant carbon source and compaction pressure, samples of different thicknesses show different kinetic behavior due to different average diameter of the carbon particles. The synergetic effect on the reaction kinetics observed for the 1/2AC-1/2G mixture as carbon source was explained based on the rheological behavior of the powder mixture during the formation process.

According to the experimental results obtained, it is possible to produce Al_2O_3/SiC nanopowder mixtures using colloidal silica and aluminum nitrate using G or 1/2AC-1/2G mixture as carbon source, 30 wt % excess stoichiometric carbon and a reaction duration of 60 min at a reaction temperature of 1500°C.

Notation

C_{SiO} = concentration of SiO in the bulk gas phase, mol m^{-3}
D_{avg} = average particle diameter, m
f = residual mullite mass divided by initial mullite mass
k = rate constant in Eq. 4, min^{-1}
k_s = rate constant of the first-order unreacted core surface reaction, m min^{-1}
k_0 = rate constant independent of temperature in the Arrhenius equation for k, m min^{-1}
L = green compact thickness, m
m_0 = weight of sample prior synthesis, g
m_c = weight of residual carbon in the synthesized product, g
R = initial average radius of carbon particles, m
S_{BET} = BET specific surface area, m^2 g^{-1}
t = reaction time, min
T = temperature, °C
ρ = density of powder, kg m^{-3}
ρ_C = density of carbon particle, kg m^{-3}

Literature Cited

Bechtold BC, Butler IB. Reaction of clay and carbon to form and separate Al_2O_3 and SiC. *J Am Ceram Soc*. 1980;63:271–275.

Berger LM, Gruner W, Lanholf E, Stolle S. On the mechanism of carbothermal reduction processes of TiO_2 and ZrO_2. *Int J Ref Met Hard Mater*. 1999;17:235–243.
Ebadzadeh T. Effects of various carbon sources on carbothermal reduction of clay. *Ind Ceram*. 2002;22:103–106.
Falamaki C, Ebadzadeh T. Kinetic investigation of the carbothermal reduction of an Iranian clay. *Ceram Int*. 2002;28:887–892.
Levenspiel O. *Chemical Reaction Engineering*. New York: Wiley Eastern, 1972: 361–368.
Martin HP, Ecke R, Mueller E. Synthesis of nanocrystalline silicon carbide powder by carbothermal reduction. *J Eur Ceram Soc*. 1998;18: 1737–1742.
Na SH. Method for manufacturing an alumina-silicon carbide nanocomposite. US Pat. 5,894,008, 1999.
Rodriguez J, Martin A, Pastor JY, Llorca J. Sliding wear of alumina/silicon carbide nano-composites. *J Am Ceram Soc*. 1999;82:2252–2254.
Weimer AW, Nielsen KJ, Cochran GA, Roach RP. Kinetics of carbothermal reduction synthesis of beta silicon carbide. *AIChE J*. 1993; 39:493–503.

Manuscript received Jan. 17, 2009, and revision received Apr. 7, 2009.